Open access • Journal Article • DOI:10.1021/JE800316B

Measurements and Correlation of High-Pressure Densities of Imidazolium-Based Ionic Liquids — Source link

Luciana I.N. Tomé, Pedro J. Carvalho, Mara G. Freire, Isabel M. Marrucho ...+4 more authors

Institutions: University of Coimbra

Published on: 19 Jul 2008 - Journal of Chemical & Engineering Data (American Chemical Society)

Topics: Tait equation, Equation of state, Ionic liquid and Compressibility

Measurements and Correlation of High-Pressure Densities of Imidazolium-Based Ionic Liquids

Luciana I. N. Tomé,[†] Pedro J. Carvalho,[†] Mara G. Freire,[†] Isabel M. Marrucho,[†] Isabel M. A. Fonseca,[‡] Abel G. M. Ferreira,[‡],* João A. P. Coutinho,[†] and Ramesh L. Gardas[†]

CICECO, Departamento de Química, Universidade de Aveiro, 3810-193 Aveiro, Portugal, and Departamento de Engenharia Química, Faculdade de Ciências a Tecnologia, Universidade de Coimbra, Polo II, Pinhal de Marrocos, 3030-290 Coimbra, Portugal

In the present work, experimental density measurements are reported along with the derived thermodynamic properties, such as the isothermal compressibility (κ_T), the isobaric expansivity (α_p), and the thermal pressure coefficient (γ_v) for imidazolium-based ionic liquids (ILs), namely, 1-ethyl-3-methylimidazolium methylsulfate [C_2mim][$MeSO_4$], 1-ethyl-3-methylimidazolium ethylsulfate [C_2mim][$EtSO_4$], 1,3-diethylimidazolium bis(trifluoromethylsulfonyl)imide [C_2eim][Tf_2N], and 1-decyl-3-methylimidazolium bis(trifluoromethylsulfonyl)imide [C_{10}mim][Tf_2N] in the pressure ($0.10 < P/\text{MPa} < 35.00$) and temperature ($293.15 < T/\text{K} < 393.15$) domains. It is shown that experimental densities are in good agreement with the predicted densities obtained by the Gardas and Coutinho method and the correlation using the Tait equation and Sanchez–Lacombe equation of state.

Introduction

Ionic liquids (ILs), in general, are the combination of large organic cations with various alkyl substituents and inorganic or organic anions, so that a very large number of ILs are possible. To better understand the nature of ionic liquids and rationally expand their applications, knowledge of their physical properties is required. The design of industrial processes and new products based on ILs can only be achieved when their thermophysical properties are adequately characterized.

High-pressure density data of pure ionic liquids available in the literature[1–22] are summarized in Table 1. This paper is a continuation of previous works[8,10,18] on high-pressure densities and derived thermodynamic properties of ILs. In this work, the experimental measurements of the pressure ($0.10 < P/\text{MPa} < 35.00$) and temperature ($293.15 < T/\text{K} < 393.15$) dependence of the density of imidazolium-based ionic liquids (ILs), namely, 1-ethyl-3-methylimidazolium methylsulfate [C_2mim][$MeSO_4$], 1-ethyl-3-methylimidazolium ethylsulfate [C_2mim][$EtSO_4$], 1,3-diethylimidazolium bis(trifluoromethylsulfonyl)imide [C_2eim][Tf_2N], and 1-decyl-3-methylimidazolium bis(trifluoromethylsulfonyl)imide [C_{10}mim][Tf_2N], are presented. The experimental densities were correlated with the Tait equation[23] and the Sanchez–Lacombe equation of state (S-L EoS)[24] and compared against the estimation method proposed by Gardas and Coutinho.[25] Derived thermodynamic properties, such as the isothermal compressibility (κ_T), the isobaric expansivity (α_p), and the thermal pressure coefficient (γ_v) are reported as Supporting Information.

The objective of this work is to contribute to the databank of thermodynamic properties of pure ILs and to investigate the relationship between densities and the ionic structures, in order to establish principles for the molecular design of ILs. For that purpose, the [C_2mim] cation was studied in combination with two anions, [$MeSO_4$] and [$EtSO_4$], to conclude about the anion effect. The volumetric study of [C_2eim][Tf_2N] and [C_{10}mim][Tf_2N] is made possible by the comparison with our previous study,[10] to understand the effect of alkyl chain length on the imidazolium ring on the density and derived properties. The effect of alkyl chain length on the imidazolium-based ILs, having the [Tf_2N] anion, on the density and derived properties has been studied.

Experimental Section

Materials. Experimental densities were measured for imidazolium-based ILs, namely, [C_2mim][$MeSO_4$], [C_2mim][$EtSO_4$], [C_2eim][Tf_2N], and [C_{10}mim][Tf_2N]. All ILs were acquired from IoLiTec (Ionic Liquids Technologies GmbH & Co. KG, Germany) with mass fraction purities > 99 % and a bromide impurity mass fraction $< 10^{-4}$.

To reduce the water content and volatile compounds to negligible values, a vacuum (0.1 Pa) at moderate temperature (353 K) for at least 48 h was applied to all the IL samples prior to their use. The purity of each IL was checked by ^{1}H, ^{13}C, and ^{19}F NMR, and the water content in the ILs was determined with a Metrohm 831 Karl Fischer coulometer indicating very low levels of water mass fraction content, as $(136, 191, 95, \text{and } 118)\cdot 10^{-6}$ for [C_2mim][$MeSO_4$], [C_2mim][$EtSO_4$], [C_2eim][Tf_2N], and [C_{10}mim][Tf_2N], respectively. The analyte used for the coulometric Karl Fischer titration was Hydranal-Coulomat AG from Riedel-de Haën.

Experimental Procedure. Experimental densities were measured using an Anton Paar DMA 60 digital vibrating tube densimeter, with a DMA 512P measuring cell in the temperature range (293.15 to 393.15) K and pressure range (0.10 to 35.00) MPa. The temperature in the vibrating tube cell was measured with a platinum resistance probe which has a temperature uncertainty of ± 0.01 K coupled with a GW instek dual display digital multimeter GDM-845. A Julabo P-5 thermostatic bath with silicone oil as circulating fluid was used in

---

* To whom correspondence should be addressed. E-mail: abel@eq.uc.pt.
[†] Universidade de Aveiro.
[‡] Universidade de Coimbra.

10.1021/je800316b CCC: $40.75

Table 1. High-Pressure Density Data of Pure Ionic Liquids Reported in the Literature

ionic liquid	*T*/K	maximum *P*/MPa	method[a]	data points	ref
$[C_4mim][PF_6]$	298.2 to 343.2	200	U	20	1
	298.15 to 323.15	100	V	144	2
	293.15 to 353.15	20	D	20	3
	298.15 to 398.15	40	V	45	4
	293.48 to 414.94	40	V	46	5
	294.9 to 335.1	20	D	09	6
	312.8 to 472.3	200	D	189	7
$[C_6mim][PF_6]$	293.15 to 393.15	10	V	77	8
	294.9 to 335.2	20	D	09	6
	293.15 to 353.15	20	D	20	9
$[C_8mim][PF_6]$	298.2 to 343.2	202	U	20	1
	293.15 to 393.15	10	V	77	8
	295.1 to 335.2	20	D	09	6
	293.15 to 353.15	20	D	20	9
$[C_2mim][BF_4]$	293.15 to 393.15	30	V	96	10
$[C_4mim][BF_4]$	278.15 to 333.15	60	V	26	11
	298.34 to 332.73	60	V	67	2
	293.15 to 353.15	20	D	20	3
	298.15 to 398.15	40	V	45	4
	293.15 to 393.15	10	V	77	8
	293.49 to 414.93	40	V	46	5
	273.15 to 348.15	300	V	62	12
	313.1 to 472.2	200	D	189	7
	298.15 to 398.15	40	V	45	13
$[C_8mim][BF_4]$	298.2 to 343.2	207	U	21	1
	293.15 to 393.15	10	V	77	8
$[C_4mmim][BF_4]$	313.15 to 393.15	10	V	63	8
$[C_2mim][Tf_2N]$	293.49 to 414.93	40	V	46	5
	293.15 to 393.15	30	V	96	10
$[C_3mim][Tf_2N]$	298.15 to 333.15	60	V	165	14
$[C_4mim][Tf_2N]$	298.15 to 328.20	60	V	168	15
	293.49 to 414.92	40	V	46	5
$[C_5mim][Tf_2N]$	298.15 to 333.15	60	V	165	14
$[C_6mim][Tf_2N]$	298.15 to 328.20	60	V	156	15
	298.15 to 423.15	40	V	28	16
	293.15 to 338.15	65	V	160	17
$[C_7mim][Tf_2N]$	293.15 to 393.15	30	V	96	10
$[C_8mim][Tf_2N]$	293.15 to 393.15	30	V	96	10
$[C_2mim][CF_3SO_3]$	293.15 to 393.15	35	V	91	18
$[C_4mim][CF_3SO_3]$	293.15 to 393.15	10	V	77	8
$[C_4mim][C(CN)_3]$	293.15 to 393.15	30	V	96	12
$[C_1mim][MeSO_4]$	313.15 to 333.15	25	V	34	19
$[C_2mim][EtSO_4]$	292.49 to 414.95	40	V	46	5
	283.15 to 333.15	35	V	63	20
$[C_4mim][OcSO_4]$	298.15 to 428.15	60	V	214	21
	312.9 to 472.6	200	D	178	7
[THTDP]$[Tf_2N]$	298.15 to 333.43	65	V	126	22
[THTDP][Cl]	298.13 to 333.14	65	V	134	22
[THTDP]$[CH_3COO]$	298.13 to 334.11	65	V	144	22
$[C_4py][BF_4]$	298.2 to 343.2	204	U	20	1
$[C_3mpy][Tf_2N]$	293.15 to 393.15	35	V	91	18
$[C_3mpyr][Tf_2N]$	293.15 to 393.15	35	V	91	18
$[C_4mpyr][Tf_2N]$	293.15 to 393.15	35	V	91	18
$[C_3mpip][Tf_2N]$	293.15 to 393.15	35	V	91	18

[a] D, dilatometer; V, vibrating tube density meter; U, ultrahigh-pressure density apparatus.

the thermostat circuit of the measuring cell which was held constant to ± 0.01 K.

The required pressure was generated and controlled with a Pressure Generator model 50-6-15, High Pressure Equipment Co., using acetone as the hydraulic fluid. The diameter of metallic tube is $1.59 \cdot 10^{-3}$ m, and the buffer is more than 1 m long which guarantees the inexistence of diffusion of the hydraulic liquid in the liquid contained in the cell of the densimeter. Pressures were measured with a pressure transducer (Wika Transmitter S-10, WIKA Alexander Wiegand GmbH & Co.) with a maximum uncertainty of ± 0.03 MPa. An NI PCI-6220 data acquisition board (DAQ) from National Instruments (NI) was used for the real time registration of values of period, temperature, and pressure. Modules of temperature (NI SCC-FT01) and pressure (NI SCC-CI20) were installed into a NI SC-2345 carrier and connected to the DAQ board.

The calibration of the vibrating tube densimeter was described in a previous work of Gardas et al.[26] The equation proposed by Niesen[27] which has a solid theoretical basis as discussed by Holcom and Outcalt[28] was used for that purpose. The standard deviation of the fitting is in the order of $\pm 1\ \mathrm{kg \cdot m^{-3}}$. The average absolute relative deviation, AARD, from the experimental data to the fitting is 0.06 % for all the ILs studied.

The influence of the viscosity on the densities was evaluated. To check the effect of viscosity in the density, a viscosity correction for compounds with viscosities $< 100\ \mathrm{mPa \cdot s}$ was applied with the equation proposed for the density uncertainty of an Anton Paar DMA 512 densimeter.[29] For compounds with viscosities higher than $400\ \mathrm{mPa \cdot s}$, the correction factor becomes constant[30] and equal to $0.5\ \mathrm{kg \cdot m^{-3}}$, and between (100 and 400) $\mathrm{mPa \cdot s}$, the viscosity correction follows an intermediate behavior. Considering, for example, the available viscosity data for $[C_2mim][EtSO_4]$[31–33] at atmospheric pressure and temperature in the range (298.15 to 343.15) K, where the viscosity of ILs is $< 100\ \mathrm{mPa \cdot s}$, allowed us to calculate an average density uncertainty less than $0.5\ \mathrm{kg \cdot m^{-3}}$. For other ILs and/or other higher pressures where the viscosity increases, the correction value was assumed as $0.5\ \mathrm{kg \cdot m^{-3}}$, being less than the uncertainty in the overall density data, which is $1\ \mathrm{kg \cdot m^{-3}}$, and for that reason viscosity corrections were neglected in the present work.

Results and Discussion

Density measurements were carried out at temperatures ranging from (293.15 to 393.15) K and pressures from (0.10 to 35.00) MPa. The experimental pressure−volume−temperature (PVT) data obtained are reported in Table 2 for all the ILs studied.

Density data for $[C_2mim][EtSO_4]$ are already available in the open literature but at atmospheric pressure[31–35] except the data by Jacquemin et al.[5] and Hofman et al.[20] The relative deviations between the experimental and literature density data of $[C_2mim][EtSO_4]$ are presented in Figure 1. Experimental data for $[C_2mim][EtSO_4]$ are in good agreement with available literature values, the relative deviations ranging from (−0.64 to 1.27) % at atmospheric pressure and up to 2 % at high pressures. It is worth noting that the experimental density data of $[C_2mim][EtSO_4]$ are in excellent agreement (within 0.15 %) with the values of Krummen et al.,[34] while they are higher (within 1.27 %) than the values of Gomez et al.,[30] Rodriguez et al.,[32] and Gonzalez et al.[33] The relative deviations from the values of Jacquemin et al.[5] show both negative and positive values (ranging from −0.64 % to 0.48 %) at atmospheric pressure and (ranging from −2.00 % to 0.36 %) at higher pressure. The literature values of densities for this analysis were obtained using the Tait equation proposed by the authors.[5] The experimental density data of $[C_2mim][EtSO_4]$ are in good agreement (percentage deviations ranging from 0.47 % to 0.71 %) with the values of Hofman et al.[20] These deviations can be due essentially to the purity of IL including water and halide content and also from the experimental technique adopted. To the best of our knowledge, no literature data on densities were previously available for $[C_2mim][MeSO_4]$, $[C_2eim][Tf_2N]$, and $[C_{10}mim][Tf_2N]$.

From the experimental densities for ILs having the $[Tf_2N]^-$ anion (comparison of $[C_2eim][Tf_2N]$ and $[C_{10}mim][Tf_2N]$) and by the comparison of densities of $[C_2eim][Tf_2N]$ with that of $[C_2mim][Tf_2N]$ from our previous paper,[10] it is observed that as the alkyl chain length in the imidazolium cation increases the density of the corresponding IL decreases. Figure 2 shows

Table 2. Experimental Density, ρ, Data for $[C_2mim][MeSO_4]$, $[C_2mim][EtSO_4]$, $[C_2eim][Tf_2N]$, and $[C_{10}mim][Tf_2N]$ as a Function of Temperature and Pressure

	ρ/kg·m^{-3} at T/K							
p/MPa	293.15	298.15	303.15	313.15	333.15	353.15	373.15	393.15
	$[C_2mim][MeSO_4]$							
0.10	1292.1	1288.0	1283.3	1276.6	1260.9	1245.5	1231.4	1218.1
2.50	1293.0	1289.1	1284.3	1277.8	1262.3	1247.5	1232.8	1219.2
5.00	1294.0	1290.1	1285.4	1278.9	1263.4	1248.7	1234.0	1220.5
7.50	1295.0	1291.1	1286.4	1279.9	1264.5	1249.9	1235.2	1221.8
10.00	1296.0	1292.1	1287.4	1281.0	1265.6	1251.1	1236.4	1223.1
15.00	1298.0	1294.1	1289.5	1283.0	1267.8	1253.4	1238.8	1225.5
20.00	1299.9	1296.1	1291.4	1285.1	1269.9	1255.6	1241.2	1227.9
25.00	1301.8	1298.0	1293.4	1287.1	1272.0	1257.8	1243.5	1230.3
30.00	1303.7	1300.0	1295.3	1289.1	1274.0	1260.0	1245.7	1232.6
35.00	1305.6	1301.9	1297.3	1291.1	1276.1	1262.2	1248.0	1234.9
	$[C_2mim][EtSO_4]$							
0.10	1246.9	1244.3	1240.8	1233.1	1218.3	1204.2	1190.1	1176.6
2.50	1249.0	1245.2	1241.6	1234.0	1219.2	1205.3	1191.3	1178.0
5.00	1250.2	1246.3	1242.7	1235.1	1220.4	1206.6	1192.6	1179.3
7.50	1251.3	1247.4	1243.8	1236.2	1221.6	1207.8	1193.9	1180.7
10.00	1252.3	1248.4	1244.9	1237.3	1222.7	1209.0	1195.2	1182.0
15.00	1254.3	1250.6	1247.0	1239.5	1225.0	1211.4	1197.7	1184.6
20.00	1256.5	1252.7	1249.1	1241.6	1227.2	1213.8	1200.2	1187.2
25.00	1258.5	1254.8	1251.1	1243.7	1229.3	1216.1	1202.6	1189.7
30.00	1260.5	1256.6	1253.2	1245.8	1231.5	1218.4	1204.9	1192.2
35.00	1262.4	1258.7	1255.2	1247.9	1233.6	1220.6	1207.3	1194.6
	$[C_2eim][Tf_2N]$							
0.10	1469.2	1463.2	1457.7	1447.3	1425.7	1404.5	1384.1	1364.2
2.50	1471.1	1465.5	1460.1	1449.6	1428.2	1407.5	1386.9	1367.2
5.00	1473.1	1467.6	1462.1	1451.6	1430.4	1409.9	1389.5	1369.9
7.50	1475.0	1469.5	1463.9	1453.7	1432.6	1412.2	1391.9	1372.5
10.00	1476.9	1471.4	1466.1	1455.8	1434.8	1414.5	1394.4	1375.1
15.00	1480.8	1475.3	1469.8	1459.7	1439.1	1419.0	1399.1	1380.2
20.00	1484.2	1479.0	1473.6	1463.5	1443.2	1423.4	1403.7	1384.9
25.00	1487.9	1482.5	1477.1	1467.2	1447.2	1427.5	1408.1	1389.6
30.00	1491.5	1486.1	1480.9	1470.9	1450.9	1431.6	1412.4	1394.3
35.00	1495.2	1489.5	1484.3	1474.6	1454.8	1435.6	1416.7	1398.6
	$[C_{10}mim][Tf_2N]$							
0.10	1282.4	1278.0	1273.6	1265.3	1245.5	1228.6	1209.6	1191.8
2.50	1285.6	1280.8	1276.4	1267.3	1247.7	1230.9	1212.4	1195.8
5.00	1287.4	1282.7	1278.3	1269.3	1249.8	1233.2	1214.8	1198.3
7.50	1289.3	1284.6	1280.3	1271.3	1251.9	1235.5	1217.3	1200.9
10.00	1291.1	1286.4	1282.1	1273.2	1254.0	1237.6	1219.6	1203.4
15.00	1294.6	1290.0	1285.8	1277.0	1258.0	1242.0	1224.2	1208.2
20.00	1298.1	1293.5	1289.4	1280.7	1261.9	1246.2	1228.6	1212.8
25.00	1301.4	1297.0	1292.9	1284.2	1265.7	1250.2	1232.9	1217.3
30.00	1304.7	1300.3	1296.3	1287.7	1269.4	1254.1	1237.0	1221.7
35.00	1308.0	1303.6	1299.6	1291.1	1273.0	1257.9	1241.1	1225.9

a comparison of the molar volumes obtained for the series of $[C_nmim][Tf_2N]$ (this work and refs 10, 14, and 15) at two temperatures, (298.15 and 323.15) K, indicating linear trends with slopes in close agreement with the one anticipated by Esperança et al.[14] and Gardas et al.[10] The variation of the molar volume per addition of one carbon atom in the alkyl chain ($\partial V_m/\partial n$) is, respectively, [(17.1 ± 0.5) and (17.4 ± 0.5)] $cm^3 \cdot mol^{-1}$ at temperatures (298.15 and 323.15) K. The change in molar volume by the addition of the $-CH_2$ group, in $[C_2mim][Tf_2N]$ to give $[C_2eim][Tf_2N]$, is obtained as 19.6 $cm^3 \cdot mol^{-1}$ at 298.15 K which is slightly higher (12.8 %) than that observed for a series of $[C_nmim][Tf_2N]$ ILs. Inversely, as expected, for ILs having a similar cation, e.g., $[C_2mim]^+$, the change in molar volume by the addition of a $-CH_2$ group in the anion of IL $[C_2mim][MeSO_4]$ to give $[C_2mim][EtSO_4]$ is 17.3 $cm^3 \cdot mol^{-1}$ at 298.15 K which is similar to that observed for the addition of a $-CH_2$ group in the cation for a series of $[C_nmim][Tf_2N]$ ILs. The molar volumes of $[C_2mim]^+$ increase with the effective anion size from $[MeSO_4] < [EtSO_4]$ and by taking into account the results of our previous papers[10] show the trend $[BF_4] < [MeSO_4] < [EtSO_4] < [Tf_2N]$.

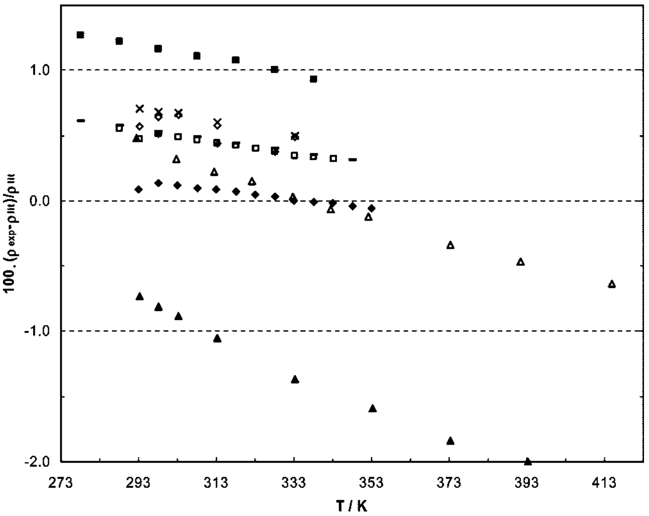

Figure 1. Relative deviations between the experimental density data of $[C_2mim][EtSO_4]$ and those reported in the literature as a function of temperature at 0.10 MPa: Δ, Jacquemin et al.;[5] ◇, Hofman et al.;[20] □, Gomez et al.;[31] −, Rodriguez et al.;[32] +, Gonzalez et al.;[33] ◆, Krummen et al.;[34] ■, Yang et al.[35] At 35.00 MPa: ▲, Jacquemin et al.;[5] ×, Hofman et al.[20]

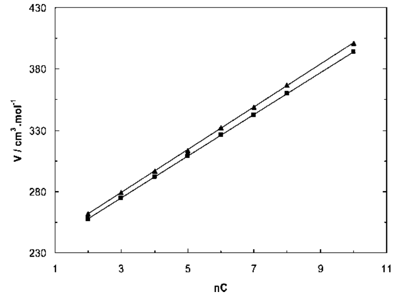

Figure 2. Molar volumes at $P = 0.1$ MPa as a function of the number of carbons, nC, on the series of $[C_nmim][NTf_2]$ (this work and references 10, 14, and 15): ■, 298.15 K; ▲, 323.15 K.

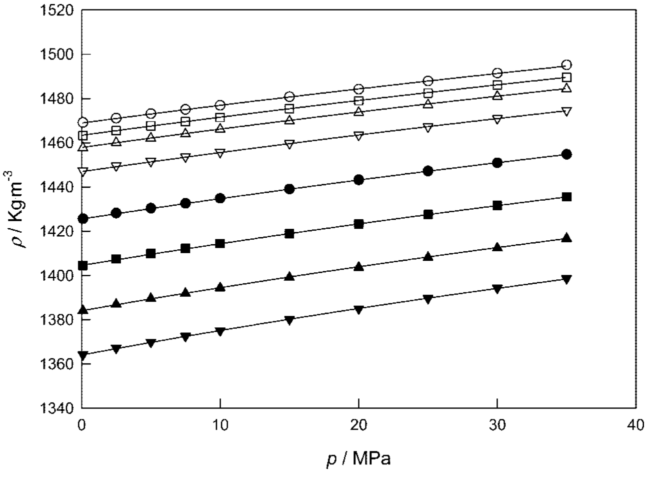

Figure 3. Isotherms of the density, ρ, for $[C_2eim][Tf_2N]$. The symbols refer to the experimental data: ○, 293.15 K; □, 298.15 K; Δ, 303.15 K; ▽, 313.15 K; ●, 333.15 K; ■, 353.15 K; ▲, 373.15 K; ▼, 393.15 K. The curves are calculated with the Tait equation, eq 1.

Modeling

Tait Equation Correlation. The liquid densities were correlated with the Tait equation,[23] and other thermodynamic properties such as the isothermal compressibility, κ_T, the isobaric expansivity, α_p, and the thermal pressure coefficient, γ_v, were calculated and reported as Supporting Information. The results

Table 3. Coefficients of Equation 2, along with Standard Deviation of the Fit (σ)

ionic liquid	a_1 / $\text{kg}\cdot\text{m}^{-3}$	a_2 / $\text{kg}\cdot\text{m}^{-3}\cdot\text{K}^{-1}$	$a_3\cdot10^4$ / $\text{kg}\cdot\text{m}^{-3}\cdot\text{K}^{-2}$	σ / $\text{kg}\cdot\text{m}^{-3}$
$[C_2\text{mim}][\text{MeSO}_4]$	1593.502	−1.2430	7.3195	0.42
$[C_2\text{mim}][\text{EtSO}_4]]$	1487.495	−0.8972	2.6966	0.48
$[C_2\text{eim}][\text{Tf}_2\text{N}]$	1845.795	−1.4624	6.036	0.25
$[C_{10}\text{mim}][\text{Tf}_2\text{N}]$	1546.69	−0.8939	−0.2304	0.77

Table 4. Coefficients of Equations 1 and 3, along with Standard Deviation of the Fit (σ) and Average Absolute Relative Deviation (AARD) of Equation 1

ionic liquid	C	b_1/MPa	$b_2\cdot10^{-4}$/MPa·K	σ/kg·m^{-3}	AARD/%
$[C_2\text{mim}][\text{MeSO}_4]$	0.05567	−10.999	5.2634	0.42	0.027
$[C_2\text{mim}][\text{EtSO}_4]$	0.08317	9.826	6.6572	0.03	0.022
$[C_2\text{eim}][\text{Tf}_2\text{N}]$	0.06313	−37.846	4.3762	0.19	0.011
$[C_{10}\text{mim}][\text{Tf}_2\text{N}]$	0.05446	−32.401	3.4109	1.34	0.057

Table 5. Calculated Densities by using Equation 11, Molar Mass (M), Molecular Volume (V), Experimental Average Density ($\rho_{\text{exptl-av}}$), Calculated Average Density ($\rho_{\text{calcd-av}}$), and Average Absolute Relative Deviation (AARD) of Ionic Liquids

ionic liquid	M / g·mol^{-1}	V/Å^3 cation	anion	data points	$\rho_{\text{exptl-av}}$ / kg·m^{-3}	$\rho_{\text{calcd-av}}$ / kg·m^{-3}	AARD / %
$[C_2\text{mim}][\text{MeSO}_4]$	222.26	182	106[a]	80	1268.7	1266.0	0.38
$[C_2\text{mim}][\text{EtSO}_4]$	236.29	182	134[a]	80	1226.2	1226.7	0.30
$[C_2\text{eim}][\text{Tf}_2\text{N}]$	405.34	210	248	80	1440.0	1451.9	0.83
$[C_{10}\text{mim}][\text{Tf}_2\text{N}]$	503.52	406	248	80	1259.6	1263.0	0.28

[a] Calculated in this work.

show that the Tait equation correlates well the pure ILs studied with an average absolute relative deviation (AARD) inferior to 0.06 %.

The following form of the Tait equation[23]

$$\rho = \frac{\rho(T,P = 0.1\ \text{MPa})}{\left\{1 - C\ln\dfrac{(B+P)}{(B+0.1)}\right\}} \tag{1}$$

where

$$\rho(T,P = 0.1\ \text{MPa}) = a_1 + a_2T + a_3T^2 \tag{2}$$

was fitted to the density data. In eq 2, a_1, a_2, and a_3 were found by fitting to the experimental $\rho(T, P = 0.1\ \text{MPa})$ and are given in Table 3.

Coefficient B is defined as

$$B = b_1 + \frac{b_2}{T} \tag{3}$$

The coefficients C, b_1, and b_2 were obtained by fitting the Tait equation to experimental data, and their values along with standard deviation σ of fit are given in Table 4. The standard deviation is defined by

$$\sigma = \left[\sum_{i=1}^{N_\text{p}} (\rho_\text{calcd} - \rho_\text{exptl})_i^2/(N_\text{p} - k)\right]^{1/2} \tag{4}$$

where N_p represents the number of data points ($N_\text{p} = 80$) and k is the number of adjusted parameters ($k = 3$). The average absolute relative deviation (AARD) was defined as

$$\text{AARD} = \frac{\sum_{i=1}^{N_\text{p}} |(\rho_\text{calcd} - \rho_\text{exptl})/\rho_\text{exptl}|_i}{N_\text{p}} \tag{5}$$

and is listed in Table 4. Figure 3 shows the good agreement between the experimental density data for $[C_2\text{eim}][\text{Tf}_2\text{N}]$ and isotherms obtained with the Tait equation.

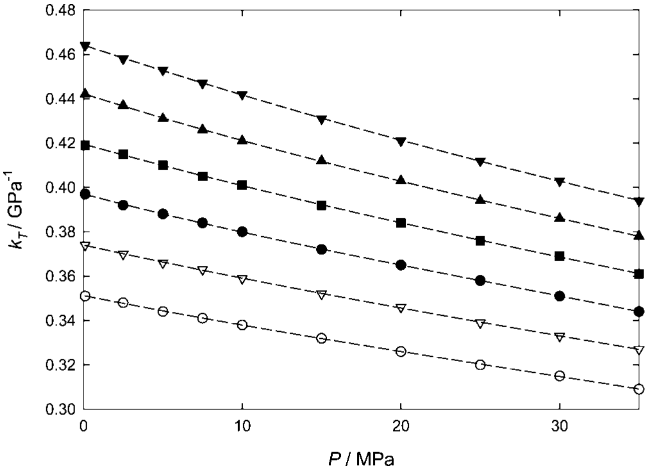

Figure 4. Isotherms for the isothermal compressibility of $[C_2\text{mim}][\text{EtSO}_4]$: ○, 293.15 K; □, 298.15 K; △, 303.15 K; ▽, 313.15 K; ●, 333.15 K; ■, 353.15 K; ▲, 373.15 K; ▼, 393.15 K. The curves were fitted to data.

The Tait equation is an integrated form of an empirical equation representative of the isothermal compressibility behavior versus pressure. The effect of pressure in density can be best described by the isothermal compressibility, κ_T, which is calculated according to the following expression

$$\kappa_T = -\frac{1}{V_\text{m}}\left(\frac{\partial V_m}{\partial P}\right)_T = \frac{1}{\rho}\left(\frac{\partial \rho}{\partial P}\right)_T = \left(\frac{\partial \ln \rho}{\partial P}\right)_T \tag{6}$$

where ρ is the density and P the pressure at constant temperature, T. The isothermal compressibilities can be calculated using eqs 1 and 6

$$\kappa_T = \left(\frac{C}{B+P}\right)\left(\frac{\rho}{\rho(T,P = 0.1\ \text{MPa})}\right) \tag{7}$$

For illustration purposes, the isothermal compressibilities of $[C_2\text{mim}][\text{EtSO}_4]$ are shown in Figure 4. The ILs become more compressible with increasing temperatures and less compressible with increasing pressure. The calculated values of κ_T are presented in the Supporting Information, as Table ST1. In the studied range of temperature, (293.15 to 393.15) K, and pressure, (0.10 to 35.00) MPa, the isothermal compressibility ranges in GPa^{-1} are 0.28 to 0.45, 0.31 to 0.46, 0.44 to 0.86, and 0.47 to 1.00, respectively, for $[C_2\text{mim}][\text{MeSO}_4]$, $[C_2\text{mim}][\text{EtSO}_4]$, $[C_2\text{eim}][\text{Tf}_2\text{N}]$, and $[C_{10}\text{mim}][\text{Tf}_2\text{N}]$.

The isobaric expansivity, α_P, is defined as

$$\alpha_P = \frac{1}{V_\text{m}}\left(\frac{\partial V_\text{m}}{\partial T}\right)_P = -\frac{1}{\rho}\left(\frac{\partial \rho}{\partial T}\right)_P = -\left(\frac{\partial \ln \rho}{\partial T}\right)_P \tag{8}$$

and the following expression is derived from the Tait equation, eq 1

$$\alpha_P = -\left\{\frac{[\text{d}\rho(T,P = 0.1\ \text{MPa})/\text{d}T]}{\rho(T,P = 0.1\ \text{MPa})}\right\} + C\left\{\frac{\dfrac{\text{d}B}{\text{d}T}(P - 0.1)}{\left[1 - \text{C}\ln\left(\dfrac{B+P}{B+0.1}\right)\right](B+0.1)(B+P)}\right\} \tag{9}$$

where $\text{d}B/\text{d}T = -b_2/T^2$. The values of α_P are presented in the Supporting Information, as Table ST2, for all investigated ILs.

The α_p values for $[C_{10}\text{mim}][\text{Tf}_2\text{N}]$ are shown in Figure 5. Studied ILs do not expand notably with temperature. However, there are some ILs that present a more significant

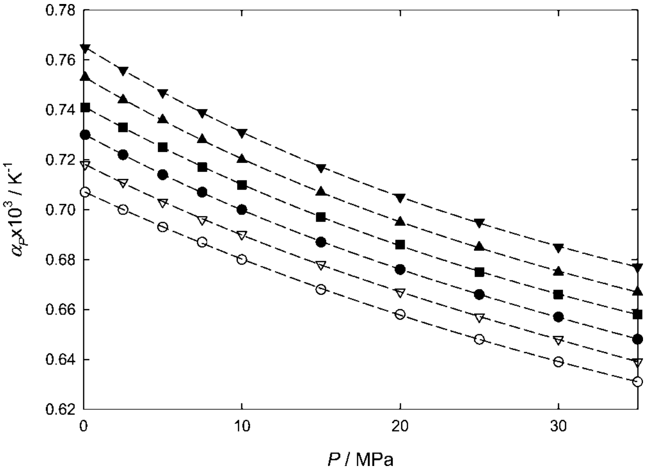

Figure 5. Isotherms for the isobaric expansivity of [C_{10}mim][Tf_2N]: ○, 293.15 K; □, 298.15 K; Δ, 303.15 K; ▽, 313.15 K; ●, 333.15 K; ■, 353.15 K; ▲, 373.15 K; ▼, 393.15 K. The curves were fitted to data.

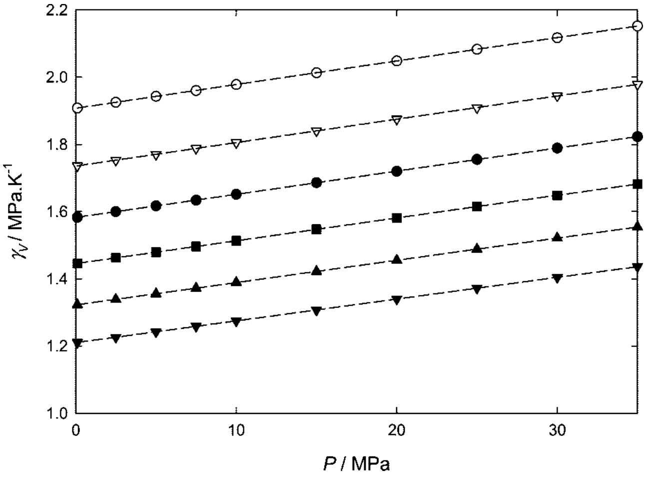

Figure 6. Isotherms for the thermal pressure coefficient of [C_2mim][$MeSO_4$]: ○, 293.15 K; □, 298.15 K; Δ, 303.15 K; ▽, 313.15 K; ●, 333.15 K; ■, 353.15 K; ▲, 373.15 K; ▼, 393.15 K. The curves were fitted to data.

decreases in α_p with temperature,[36] but in fact, ILs do not expand markedly with temperature and have α_p values lower than most organic liquids and similar to that of water. From eq 9, the isobaric expansivity, for the studied range of temperature (293.15 to 393.15) K and pressure (0.10 to 35.00) MPa, is $\{(0.5 \text{ to } 0.6)\cdot 10^{-3}$, $(0.5 \text{ to } 0.6)\cdot 10^{-3}$, $(0.6 \text{ to } 0.8)\cdot 10^{-3}$, and $(0.6 \text{ to } 0.8)\cdot 10^{-3}\}$ K^{-1}, respectively, for [C_2mim][$MeSO_4$], [C_2mim][$EtSO_4$], [C_2eim][Tf_2N], and [C_{10}mim][Tf_2N].

The thermal pressure coefficient, γ_V, may be calculated according to

$$\gamma_V = \frac{\alpha_p}{\kappa_T} \tag{10}$$

The thermal pressure coefficients as a function of pressure obtained for investigated ILs are shown in Figure 6 for [C_2mim][$MeSO_4$]. The γ_V decreases with temperature and increases slightly with pressure for all the ILs studied (see Supporting Information, Table ST3). We have applied the propagation law of errors at eqs 7, 9, and 10 taking into account the uncertainties in the parameters c, b_1, and b_2 of the Tait equation, eq 1, and a_1 to a_3 of eq 2, and also in the temperature and pressure. We have concluded that the uncertainty in κ_T was of the order of ± 0.05 GPa^{-1}, while for α_p it will be of the order of ± $5\cdot 10^{-4}$ K^{-1}. The uncertainty in γ_V was determined with the law of propagation of errors from the uncertainty in α_p and κ_T. We have obtained a maximum uncertainty of ± 1 MPa·K^{-1}, which is almost of the same magnitude of the thermal pressure coefficient.

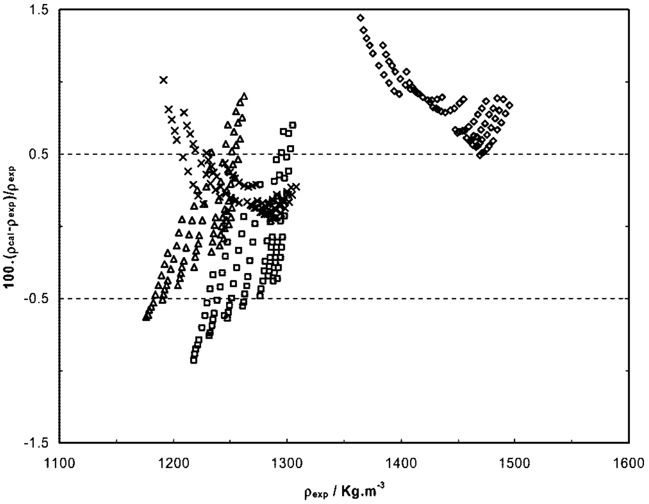

Figure 7. Relative deviations between the experimental and calculated density using eq 11 as a function of experimental density of ionic liquids: □, [C_2mim][$MeSO_4$]; Δ, [C_2mim][$EtSO_4$]; ◇, [C_2eim][Tf_2N]; ×, [C_{10}mim]-[Tf_2N].

Correlation by the Gardas and Coutinho Estimation Method. Recently, we proposed a new method[25] for the estimation of ionic liquid densities in a wide range of temperatures, (273.15 to 393.15) K, and pressures, (0.10 to 100) MPa, according to eq 11

$$\rho = \frac{M}{NV(a + bT + cP)} \tag{11}$$

where ρ is the density in kg·m^{-3}; M is molar mass in kg·mol^{-1}; N is the Avogadro constant; V is the molecular volume in Å^3; T is the temperature in K; and P is the pressure in MPa. The coefficients a, b, and c were estimated by fitting eq 11 to our previously published experimental data.[8,10] A total amount of ca. 800 density data points were used. The values of coefficient a, b, and c obtained are $8.005\cdot 10^{-1} \pm 2.333\cdot 10^{-4}$, $(6.652\cdot 10^{-4} \pm 6.907\cdot 10^{-7})$ K^{-1}, and $(-5.919\cdot 10^{-4} \pm 2.410\cdot 10^{-6})$ MPa^{-1}, respectively, at 95 % confidence level. The average absolute relative deviation of calculated densities from the experimental densities is 0.29 %. The experimental density (Y) for the ILs used to obtain coefficients a, b, and c of eq 11 is essentially identical to its calculated density (X): $Y = (0.9998 \pm 0.0003)X$ (correlation coefficient: $R^2 = 0.9989$, at 95 % level of confidence). For the density calculation, volume parameters (V) of ions and groups were either directly taken from the literature[37] or calculated following the Jenkins procedure.[38] The volume of the sulfate anion (SO_4^{-2}) is estimated in this work as 71 Å^3 by minimizing the objective function (O.F.)

$$\text{O.F.} = \frac{\sum_{i=1}^{N_p} |(\rho_{\text{calcd}} - \rho_{\text{exptl}})/\rho_{\text{exptl}}|_i}{N_p} \tag{12}$$

where N_p represents the number of data points (N_p = 160) of [C_2mim][$MeSO_4$] and [C_2mim][$EtSO_4$].

Table 6. Sanchez−Lacombe Equation of State Parameters, Characteristic Pressure (P^*), Temperature (T^*), and Density (ρ^*), Segment Number of One Molecule (r), Segment Interaction Energy (ε^*), Segment Volume (ν^*), and Hard Core Volume ($\nu^* \times r$) and Average Absolute Relative Deviation (AARD) of Ionic Liquids

ionic liquid	P^* MPa	T^* K	ρ^* kg·m^{-3}	r	ε^* J·mol^{-1}	ν^* cm^3·mol^{-1}	$\nu^* \times r$ cm^3·mol^{-1}	AARD %
[C$_2$mim][MeSO$_4$]	575.2	685.7	1359.2	16.5	5701	9.91	163.5	0.13
[C$_2$mim][EtSO$_4$]	574.3	675.2	1316.9	18.4	5614	9.78	179.4	0.15
[C$_2$eim][Tf$_2$N]	498.0	603.2	1580.4	25.5	5015	10.07	256.5	0.18
[C$_{10}$mim][Tf$_2$N]	544.7	598.4	1382.0	39.9	4975	9.13	364.3	0.20

The densities of [C$_2$mim][MeSO$_4$], [C$_2$mim][EtSO$_4$], [C$_2$eim][Tf$_2$N], and [C$_{10}$mim][Tf$_2$N] were calculated by using eq 11. Calculated densities with the average absolute relative deviation (AARD) of studied ILs are shown in Table 5. As shown in Figure 7, the experimental densities (Y) of [C$_2$mim][MeSO$_4$], [C$_2$mim][EtSO$_4$], [C$_2$eim][Tf$_2$N], and [C$_{10}$mim][Tf$_2$N] display a very good agreement with the predicted densities (X) from eq (11): $Y = (0.9972 \pm 0.0003)X$ (correlation coefficient: $R^2 = 0.9947$, at a 95 % level of confidence).

These results (Table 5 and Figure 7) show that the density estimation method proposed by Gardas and Coutinho[25] can be applied with confidence to ionic liquids from families other than those used on the development of the correlation.

Correlation by the Sanchez−Lacombe Equation of State. The Sanchez−Lacombe equation of state (S−L EoS) is based on lattice fluid theory[24] and can be used to predict phase equilibria from the pure component parameters. This equation of state is given by the following equations

$$\begin{gathered}\tilde{\rho}^2 + \tilde{P} + \tilde{T}\left[\ln(1-\tilde{\rho}) + \left(1 - \frac{1}{r}\right)\tilde{\rho}\right] = 0 \\ \tilde{\rho} \equiv \rho/\rho^* \quad \tilde{P} \equiv P/P^* \quad \tilde{T} \equiv T/T^* \\ \varepsilon^* = RT^* \quad \upsilon^* = RT^*/P^* \quad r = MP^*/RT^*\rho^* \end{gathered} \tag{13}$$

where P^*, T^*, and ρ^* represent characteristic parameters of the EOS; M is molar mass; and R is the gas constant. For studied ILs, the characteristic parameters were determined by fitting the equation of state (eq 13) to the experimental pressure−volume−temperature (PVT) data in the region from (293 to 393) K and from (0.1 to 35) MPa.

The S−L EoS parameters and the segment number of one molecule (r), segment interaction energy (ε^*), segment volume (ν^*), and hard core volume ($\nu^* \times r$) calculated from the S−L EoS parameters are summarized in Table 6. Figure 8 shows the relative deviations between the experimental and calculated density data as a function of experimental densities, using eq 13, for studied ILs. The maximum deviation between calculated and experimental density data was within 0.53 % for all ionic liquids.

The free volume (V_f) can be calculated as

$$V_f = V_m - (\upsilon^* \times r) \tag{14}$$

where V_m is the molar volume of IL at given T and P. This equation was applied by Machida et al.[7] to determine the free volume of ILs. Figure 9 shows free volumes, calculated using eq 14, of studied ILs as a function of temperature at (0.1 and 35) MPa. As expected, the free volume of studied ILs increased with temperature and decreased with pressure. For the studied ILs, free volume is increasing showing the trend: [C$_2$mim][MeSO$_4$] < [C$_2$mim][EtSO$_4$] < [C$_2$eim][Tf$_2$N] < [C$_{10}$mim][Tf$_2$N].

Conclusions

Experimental density data for four pure ILs in the temperature range (293.15 to 393.15) K and pressure range (0.10 to 35.00) MPa are presented. Density results can be explained by structural variations in the cation and anion. From the experimental data, a proportional molar volume increase with the alkyl chain length of the cation of ILs was observed. The liquid densities were correlated with the Tait equation[23] that has shown to describe well all the pure ILs studied with an average absolute relative deviation (AARD) less than 0.06 %.

The experimental results were also used to estimate some derivative thermodynamic properties such as the isothermal compressibility, the isobaric expansivity, and the thermal

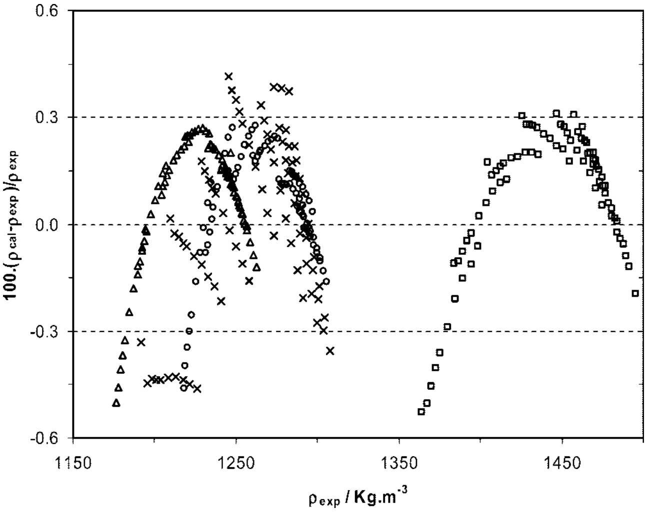

Figure 8. Relative deviations between the experimental and calculated density using eq 13 as a function of experimental density of ionic liquids: □, [C$_2$mim][MeSO$_4$]; Δ, [C$_2$mim][EtSO$_4$]; ○, [C$_2$eim][Tf$_2$N]; ×, [C$_{10}$mim]-[Tf$_2$N].

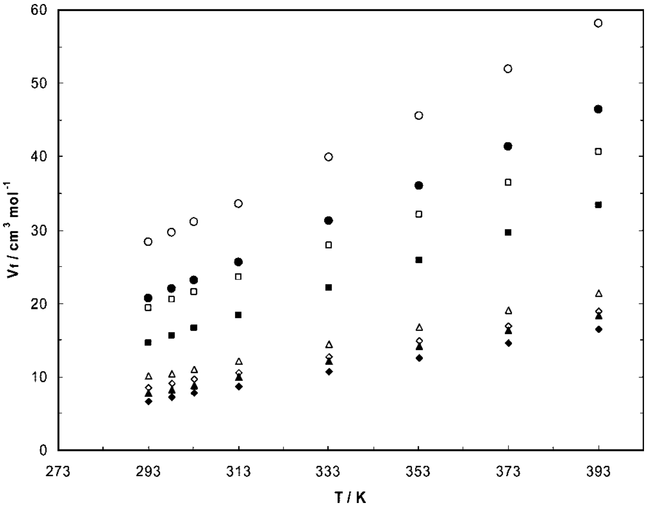

Figure 9. Free volume of investigated ionic liquids, [C$_2$mim][MeSO$_4$]: ◇, 0.1 MPa; ◆, 35 MPa. [C$_2$mim][EtSO$_4$]: Δ, 0.1 MPa; ▲, 35 MPa. [C$_2$eim][Tf$_2$N]: □, 0.1 MPa; ■, 35 MPa. [C$_{10}$mim][Tf$_2$N]: ○, 0.1 MPa; ●, 35 MPa.

pressure coefficient of the studied ILs that are difficult to obtain by direct measurements at extreme conditions of pressure and temperature.

The Gardas and Coutinho[25] method for the prediction of ionic liquid densities was tested against the measured densities and results showing that it applies to other ionic liquid families than those used for its development.

The Sanchez−Lacombe equation of state was used to correlate the density data of studied ionic liquids. The maximum deviation between calculated and experimental density data was within 0.53 % for all ionic liquids.

Supporting Information Available:

An additional three tables. This material is available free of charge via the Internet at http://pubs.acs.org.

Literature Cited

(1) Gu, Z.; Brennecke, J. F. Volume Expansivities and Isothermal Compressibilities of Imidazolium and Pyridinium-Based Ionic Liquids. *J. Chem. Eng. Data* **2002**, *47*, 339–345.

(2) De Azevedo, R. G.; Esperanca, J. M. S. S.; Najdanovic-Visak, V.; Visak, Z. P.; Guedes, H. J. R.; Ponte, M. N. D.; Rebelo, L. P. N. Thermophysical and thermodynamic properties of 1-butyl-3-methylimidazolium tetrafluoroborate and 1-butyl-3-methylimidazoliuin hexafluorophosphate over an extended pressure range. *J. Chem. Eng. Data* **2005**, *50*, 997–1008.

(3) Tomida, D.; Kumagai, A.; Qiao, K.; Yokoyama, C. Viscosity of [bmim][PF$_6$] and [bmim][BF$_4$] at high pressure. *Int. J. Thermophys.* **2006**, *27*, 39–47.

(4) Tekin, A.; Safarov, J.; Shahverdiyev, A.; Hassel, E. (p, ρ, T) Properties of 1-butyl-3-methylimidazolium tetrafluoroborate and 1-butyl-3-methylimidazolium hexafluorophosphate at T = (298.15 to 398.15) K and pressures up to p = 40 MPa. *J. Mol. Liq.* **2007**, *136*, 177–182.

(5) Jacquemin, J.; Husson, P.; Mayer, V.; Cibulka, I. High-Pressure Volumetric Properties of Imidazolium-Based Ionic Liquids: Effect of the Anion. *J. Chem. Eng. Data* **2007**, *52*, 2204–2211.

(6) Tomida, D.; Kenmochi, S.; Tsukada, T.; Qiao, K.; Yokoyama, C. Thermal conductivities of [bmim][PF$_6$], [hmim][PF$_6$], and [omim][PF$_6$] from 294 to 335 K at pressures up to 20 MPa. *Int. J. Thermophys.* **2007**, *28*, 1147–1160.

(7) Machida, H.; Sato, Y.; Smith, R. L., Jr. Pressure-volume-temperature (PVT) measurements of ionic liquids ([bmim$^+$][PF$_6^-$], [bmim$^+$][BF$_4^-$], [bmim$^+$][OcSO$_4^-$]) and analysis with the Sanchez-Lacombe equation of state. *Fluid Phase Equilib.* **2008**, *264*, 147–155.

(8) Gardas, R. L.; Freire, M. G.; Carvalho, P. J.; Marrucho, I. M.; Fonseca, I. M. A.; Ferreira, A. G. M.; Coutinho, J. A. P. High-pressure densities and derived thermodynamic properties of imidazolium-based ionic liquids. *J. Chem. Eng. Data* **2007**, *52*, 80–88.

(9) Tomida, D.; Kumagai, A.; Kenmochi, S.; Qiao, K.; Yokoyama, C. Viscosity of 1-hexyl-3-methylimidazolium hexafluorophosphate and 1-octyl-3-methylimidazolium hexafluorophosphate at high pressure. *J. Chem. Eng. Data* **2007**, *52*, 577–579.

(10) Gardas, R. L.; Freire, M. G.; Carvalho, P. J.; Marrucho, I. M.; Fonseca, I. M. A.; Ferreira, A. G. M.; Coutinho, J. A. P. PρT Measurements of Imidazolium-Based Ionic Liquids. *J. Chem. Eng. Data* **2007**, *52*, 1881–1888.

(11) Rebelo, L. P. N.; Najdanovic-Visak, V.; Visak, Z. P.; Nunes Da Ponte, M.; Szydlowski, J.; Cerdeirina, C. A.; Troncoso, J.; Romani, L.; Esperanca, J. M. S. S.; Gliedes, H. J. R.; De Sousa, H. C. A detailed thermodynamic analysis of [C$_4$mim][BF$_4$] + water as a case study to model ionic liquid aqueous solutions. *Green Chem.* **2004**, *6*, 369–381.

(12) Harris, K. R.; Kanakubo, M.; Woolf, L. W. Temperature and Pressure Dependence of the Viscosity of the Ionic Liquid 1-Butyl-3-methylimidazolium Tetrafluoroborate: Viscosity and Density Relationships in Ionic Liquids. *J. Chem. Eng. Data* **2007**, *52*, 2425–2430.

(13) Abdulagatov, I.; Tekin, A.; Safarov, J.; Shahverdiyev, A.; Hassel, E. Densities and Excess, Apparent, and Partial Molar Volumes of Binary Mixtures of BMIMBF4 + Ethanol as a Function of Temperature, Pressure, and Concentration. *Int. J. Thermophys*. **2008**, *29*, 505–533.

(14) Esperanca, J. M. S. S.; Visak, Z. P.; Plechkova, N. V.; Seddon, K. R.; Guedes, H. J. R.; Rebelo, L. P. N. Density, Speed of Sound, and Derived Thermodynamic Properties of Ionic Liquids over an Extended Pressure Range. 4. [C$_3$mim][NTf$_2$] and [C$_5$mim][NTf$_2$]. *J. Chem. Eng. Data* **2006**, *51*, 2009–2015.

(15) De Azevedo, R. G.; Esperanca, J. M. S. S.; Szydlowski, J.; Visak, Z. P.; Pires, P. F.; Guedes, H. J. R.; Rebelo, L. P. N. Thermophysical and thermodynamic properties of ionic liquids over an extended pressure range: [bmim][NTf$_2$] and [hmim][NTf$_2$]. *J. Chem. Thermodyn.* **2005**, *37*, 888–899.

(16) Kandil, M. E.; Marsh, K. N.; Goodwin, A. R. H. Measurement of the viscosity, density, and electrical conductivity of 1-hexyl-3-methylimidazolium bis(trifluorosulfonyl)imide at temperatures between (288 and 433) K and pressures below 50 MPa. *J. Chem. Eng. Data* **2007**, *52*, 2382–2387.

(17) Esperanca, J. M. S. S.; Guedes, H. J. R.; Lopes, J. N. C.; Rebelo, L. P., N. Pressure-Density-Temperature (p-ρ-T) Surface of [C$_6$mim][NTf$_2$]. *J. Chem. Eng. Data* **2008**, *53*, 867–870.

(18) Gardas, R. L.; Costa, H. F.; Freire, M. G.; Carvalho, P. J.; Marrucho, I. M.; Fonseca, I. M. A.; Ferreira, A. G. M.; Coutinho, J. A. P. Densities and Derived Thermodynamic Properties of Imidazolium-, Pyridinium-, Pyrrolidinium-, and Piperidinium-Based Ionic Liquids. *J. Chem. Eng. Data* **2008**, *53*, 805–811.

(19) Goldon, A.; Dabrowska, K.; Hofman, T. Densities and Excess Volumes of the 1,3-Dimethylimidazolium Methylsulfate + Methanol System at Temperatures from (313.15 to 333.15) K and Pressures from (0.1 to 25) MPa. *J. Chem. Eng. Data* **2007**, *52*, 1830–1837.

(20) Hofman, T.; Goldon, A.; Nevines, A.; Letcher, T. M. Densities, excess volumes, isobaric expansivity, and isothermal compressibility of the (1-ethyl-3-methylimidazolium ethylsulfate + methanol) system at temperatures (283.15 to 333.15) K and pressures from (0.1 to 35) MPa. *J. Chem. Thermodyn.* **2008**, *40*, 580–591.

(21) Davila, M. J.; Aparicio, S.; Alcalde, R.; Garcia, B.; Leal, J. M. On the properties of 1-butyl-3-methylimidazolium octylsulfate ionic liquid. *Green Chem.* **2007**, *9*, 221–232.

(22) Esperanca, J. M. S. S.; Guedes, H. J. R.; Blesic, M.; Rebelo, L. P. N. Densities and Derived Thermodynamic Properties of Ionic Liquids. 3. Phosphonium-Based Ionic Liquids over an Extended Pressure Range. *J. Chem. Eng. Data* **2006**, *51*, 237–242.

(23) Dymond, J. H.; Malhotra, R. The Tait equation: 100 years on. *Int. J. Thermophys.* **1988**, *9*, 941–951.

(24) Sanchez, I. C.; Lacombe, R. H. Statistical Thermodynamics of Polymer-Solutions. *Macromolecules* **1978**, *11*, 1145–1156.

(25) Gardas, R. L.; Coutinho, J. A. P. Extension of the Ye and Shreeve group contribution method for density estimation of ionic liquids in a wide range of temperatures and pressures. *Fluid Phase Equilib.* **2008**, *263*, 26–32.

(26) Gardas, R. L.; Johnson, I.; Vaz, D. M. D.; Fonseca, I. M. A.; Ferreira, A. G. M. PVT Property Measurements for Some Aliphatic Esters from (298 to 393) K and up to 35 MPa. *J. Chem. Eng. Data* **2007**, *52*, 737–751.

(27) Niesen, V. G. (Vapor + Liquid) Equilibria and Coexisting Densities of (Carbon Dioxide + n-butane) at 311 to 395 K. *J. Chem. Thermodyn.* **1990**, *22*, 777–795.

(28) Holcomb, C. D.; Outcalt, S. L. A Theoretical-Based Calibration and Evaluation Procedure for Vibrating-Tube Densimeters. *Fluid Phase Equilib.* **1998**, *150*−*151*, 815–827.

(29) Fandiño, O.; Pensado, A. S.; Lugo, L.; Comuñas, M. P. J.; Fernández, J. Compressed Liquid Densities of Squalane and Pentarythritol Tetra(2-ethylhexanoate). *J. Chem. Eng. Data* **2005**, *50*, 939–946.

(30) Fandiño, O.; Garcia, J.; Comuñas, M. P. J.; López, E. R.; Fernández, J. *PρT* Measurements and Equation of State (EoS) Predictions of Ester Lubricants up to 45 MPa. *Ind. Eng. Chem. Res.* **2006**, *45*, 1172–1182.

(31) Gomez, E.; Gonzalez, B.; Calvar, N.; Tojo, E.; Dominguez, A. Physical Properties of Pure 1-Ethyl-3-methylimidazolium Ethylsulfate and Its Binary Mixtures with Ethanol and Water at Several Temperatures. *J. Chem. Eng. Data* **2006**, *51*, 2096–2102.

(32) Rodriguez, H.; Brennecke, J. F. Temperature and Composition Dependence of the Density and Viscosity of Binary Mixtures of Water + Ionic Liquid. *J. Chem. Eng. Data* **2006**, *51*, 2145–2155.

(33) Gonzalez, E. J.; Gonzalez, B.; Calvar, N.; Dominguez, A. Physical Properties of Binary Mixtures of the Ionic Liquid 1-Ethyl-3-methylimidazolium Ethyl Sulfate with Several Alcohols at T = (298.15, 313.15, and 328.15) K and Atmospheric Pressure. *J. Chem. Eng. Data* **2007**, *52*, 1641–1648.

(34) Krummen, M.; Wasserscheid, P.; Gmehling, J. Measurement of Activity Coefficients at Infinite Dilution in Ionic Liquids Using the Dilutor Technique. *J. Chem. Eng. Data* **2002**, *47*, 1411–1417.

(35) Yang, J.-Z.; Lu, X.-M.; Gui, J.-S.; Xu, W.-G.; Li, H.-W. Volumetric properties of room temperature ionic liquid 2: The concentrated aqueous solutions of {1-methyl-3-ethylimidazolium ethyl sulfate + water} in a temperature range of 2782 to 338.2 K. *J. Chem. Thermodyn.* **2005**, *37*, 1250–1255.

(36) Ionic Liquids in the Dortmund Data Bank, http://www.ddbst.de/new/frame_ionic_liquids.htm.

(37) Ye, C.; Shreeve, J. M. Rapid and Accurate Estimation of Densities of Room-Temperature Ionic Liquids and Salts. *J. Phys. Chem. A* **2007**, *111*, 1456–1461.

(38) Jenkins, H. D. B.; Roobottom, H. K.; Passmore, J.; Glasser, L. Relationships among Ionic Lattice Energies, Molecular (Formula Unit) Volumes, and Thermochemical Radii. *Inorg. Chem.* **1999**, *38*, 3609–3620.

Received for review May 3, 2008. Accepted June 10, 2008. This work was supported by Fundação para a Ciência e a Tecnologia (Project POCI/EQU/58152/2004). R. L. Gardas, P. J. Carvalho, and M. G. Freire acknowledge the financial support from Fundação para a Ciência e a Tecnologia through, respectively, their postdoctoral (SFRH/BPD/23246/2005) and PhD. scholarships (SFRH/BD/41562/2007) and (SFRH/BD/14134/2003).

JE800316B